Available online at www.sciencedirect.com

ScienceDirect

Procedia Computer Science 180 (2021) 122–131

Procedia Computer Science

www.elsevier.com/locate/procedia

International Conference on Industry 4.0 and Smart Manufacturing

Scalable model for industrial coffee roasting chamber

Federico Di Palma[a], Francesca Iacono[b], Chiara Toffanin[b,*], Andrea Ziccardi[c], Lalo Magni[a]

[a] *Department of Civil and Architecture Engineering, University of Pavia, via Ferrata 3, Pavia, 27100, Italy*
[b] *Department of Electrical, Computer and Biomedical Engineering, University of Pavia, via Ferrata 3, Pavia, 27100, Italy*
[c] *Brambati S.p.A., Via Strada Nuova 37, Codevilla, 27050, Italy*

Abstract

The temperature profile of the coffee beans during the roasting phase determines the colour, aroma and flavour of the coffee. In order to reproduce these desired characteristics, the control of the coffee beans temperature has a key role in the roasting process. A proper model of the plant is required to design an intelligent control. Recently, several physical models that share the main physical equations have been proposed, but they have physical parameters specific of each process. In such scenario, each plant requires an ad hoc identification of the model parameters. This work proposes a model of the roasting chamber that can be used on plants of different sizes by scaling only geometrical parameters directly measurable on the roasting plant. The proposed model was identified on a 120 kg plant and then applied to a 360 kg one. The obtained results show in both cases similar accuracy (FIT = 75.49%, MPE=4.66%).

Keywords: Coffee roasting; Food processing; Heat flows; Physical model

1. Introduction

Coffee is one of the highest economic value commodity in the global market [8]. The roasting of the coffee beans is the industrial process mainly responsible for forming the flavour and aroma of a cup of coffee [1]. This process is suitable to be object of different research projects, so that the growing interest in it is not surprising: energy consumption [10], roasting temperature control [17], taste prediction [14] and even smart design with connected devices [18] are some examples of the current research applications. Several studies were conducted to model the behaviour of an industrial roasting chamber since all these applications require a model for their design and testing. A solid physical model of the whole roasting plant was provided in [13]. Some physical parameters of this model, like specific heats or transfer coefficients, are closely related to the particular coffee bean quality (like Robusto or Arabica) and the particular size of the plant (e.g. 120 kg, 360 kg or 600 kg) used to identify the model. Further studies investigated with a

* Corresponding author. Tel.: +39-0382-985354.
E-mail address: chiara.toffanin@unipv.it

10.1016/j.procs.2021.01.362

greater detail the coffee bean reaction in the chamber providing a better description of the coffee beans parameters [6], [2]. Nevertheless, the strong connection between the coffee beans quality, the size of the plant and the whole model still stands. Such connections strongly limited the application of the model to different plants, requiring de facto a new parameter identification phase each time. This is particularly relevant in food industry processes where data collection requires the consumption of a considerable amount of resources (e.g. several kg of coffee). In order to avoid food waste several strategies have been investigated, considering also advanced process control techniques [5].

This work proposes a scalable model that can be used on plants of different size. Starting from the model proposed in [13] and exploiting some considerations from [11], a first group of parameters is defined as function of the chamber geometry, while the others are identified through non linear identification. In this way the model identified with data collected on one plant can be used on plants of different sizes simply scaling the first group of parameters, without requiring a new identification phase. The methodology is validated identifying the model with data collected on a 120 kg plant and simulating the behaviour on a 360 kg one, obtaining satisfactory results.

The paper is structured as follows: Section 2 describes the industrial roasting process, while Section 3 is devoted to describe the proposed model. Section 4 illustrates the experimental setup used to collect the data. The identification procedure is described in Section 5 and Section 6 shows the results. Finally the conclusions are drawn in Section 7.

Nomenclature

A	Arrhenius equation pre-factor
A_{gb}	gas to beans heat transfer area
A_{gm}	gas to metal heat transfer area
A_{bm}	metal to beans heat transfer area
c_b	specific heat capacity of coffee beans
c_g	specific heat capacity of drying air
c_m	specific heat capacity of the metal
D_b	bean diameter
D_{ch}	chamber diameter
G_g	gas mass-flow rate
h_e	gas to beans heat transfer coefficient
h_{gm}	gas to metal heat transfer coefficient
h_{bm}	metal to beans heat transfer coefficient
H_a	activation energy
H_e	reaction heat produced thus far
H_{et}	total reaction heat
H_{flap}	flap height
k_1, k_2	Schwartzberg's semi-empirical parameters
K_t	bean temperature sensor time constant
L_{ch}	chamber length
m_b	bean mass
M_b	green beans coffee batch mass
M_{bd}	dry beans coffee batch mass
M_m	metal mass
P_{bm}	percentage of bean metal contact area
Q_e	external sources heat transfer rate
Q_{gb}	gas to beans heat transfer rate
Q_{gm}	gas to metal heat transfer rate
Q_{bm}	metal to beans heat transfer rate
Q_r	exothermic heat production
R	gas constant
S_{flap}	flap step

T_b	beans temperature
T_g	gas temperature
T_{gi}	gas inlet temperature
T_{go}	gas outlet temperature
X	beans moisture content
λ	latent heat of vaporization of beans moisture

2. Roasting process

The roasting of green coffee beans is a complex process that involves several chemical reactions fundamental to determinate the coffee colour, flavour and aroma. In particular, these characteristics are determined by the temperature profile of the coffee beans during the roasting.

The roasting process is composed by three major phases: drying, roasting and cooling. During these phases the coffee bean is subjected to heat and mass transfers. The heat transfer occurs both by convection and conduction, and increases the bean temperature with consequent physical and chemical changes, such as a mass transfer due to the evaporation of water inside the bean and exothermic reactions.

Several roaster architectures are available on the market, this work considers a batch roaster: a plant that treats only a fixed amount of coffee, called batch, throughout a single operating cycle (see Fig. 1). Each cycle is characterized by an initial phase where no coffee is loaded in the machine and both the air stream and the drum walls are heated up to the desired temperature. The process starts with a batch of green coffee beans at the environmental temperature loaded to the roaster drum through a conical funnel (7 in Fig. 1). Then, the drying phase starts when the air flow (9 in Fig. 1) heated by the furnace (1 in Fig. 1) is aspirated in the drum chamber (2 in Fig. 1) via a fan. The drum rotates at a uniform speed to ensure a uniform effect and to avoid the beans to adhere to the drum walls. The chamber is equipped with spiral blades in the internal surface to mix the beans in the axial direction. During this phase, the hot air flow dries the beans, then the beans are heated up until exothermic reactions near the end of roasting cause a rapid increase in the bean temperature rise (roasting phase). The gases leave the chamber through a cyclone (3 in Fig. 1) that removes the chaff released by the beans during the roasting process. These gases can be either collected in a stack after be passed in a afterburner (6 in Fig. 1) to be discharged (5 in Fig. 1) or in part sent back to the roaster furnace (4 in Fig. 1). Once the end-of-roast temperature is reached, the gas supply is turned off and the roasting process is stopped by spraying cool water on the beans to evaporatively cool them (8 in Fig. 1). The cooling phase proceeds in the cooling tank, where the beans are transferred to be stirred and further cooled through cold air input. Finally, the beans are unloaded and the system is prepared for the next roasting cycle. It is worth to be noted that the machine warming up phase particularly influences the roasting of the first batch [2].

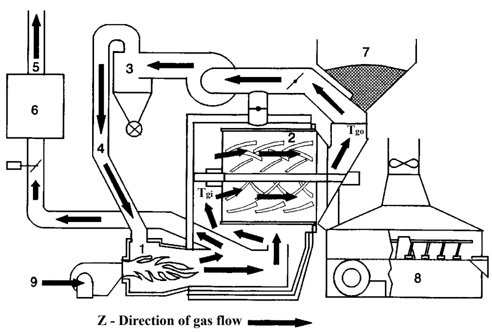

Fig. 1: Rotating-drum roaster with solid wall: 1 furnace, 2 roaster drum, 3 cyclone, 4 gas recycle line, 5 gas discharge stack, 6 catalytic afterburner, 7 green bean bin, 8 cooler, 9 fresh air. Figure from [13].

3. Model

In recent years, several models have been proposed to investigate the roasting process of the green coffee beans. In the following, the one proposed by [13] is considered and extended using considerations published in [11]. This work is focused on the adaptation of this model for a batch roaster and defines some of the model parameters on the base of the chamber geometry in order to create a new scalable model. Starting from the machine where the data were collected on, this model will be able to describe the behaviour of new different unseen machines.

3.1. Hot gas heat transfer

During the roasting process hot gas is introduced in the roasting chamber. Considering a uniform flow in a single direction and a convective heat transfer between gas and beans, a temperature balance in the Z-direction (see Fig. 1) can be expressed as:

$$-G_g c_g \frac{dT_g}{dZ} = h_e \frac{dA_{gb}}{dZ}(T_g - T_b) \tag{1}$$

where G_g is the gas mass-flow rate, c_g is the specific heat capacity of drying air, h_e is the gas to beans heat transfer coefficient, A_{gb} is the gas to beans heat transfer area, T_g and T_b are known gas and beans temperatures.
In particular, c_g is defined in [16] considering the thermophysical properties of drying air obtained from [7] as:

$$c_g = \sum_{i=0}^{6} \alpha_i (T_{gi} + 273.15)^i \tag{2}$$

where $\alpha_0 = 1.0839 \cdot 10^3$, $\alpha_1 = -7.2075 \cdot 10^{-1}$, $\alpha_2 = +2.1034 \cdot 10^{-3}$, $\alpha_3 = -2.3267 \cdot 10^{-6}$, $\alpha_4 = 1.3621 \cdot 10^{-9}$, $\alpha_5 = -4.1550 \cdot 10^{-13}$, $\alpha_6 = 5.3091 \cdot 10^{-17}$. In [13], h_e is considered a fixed parameter, on the contrary in this work it depends on the moisture quantity X, as defined in [11]:

$$h_e = 0.49 - 0.443 exp^{-0.206X} \tag{3}$$

Integrating Equation (1) between the gas inlet and outlet temperatures (T_{gi} and T_{go}) and rearranging, Equation (4) is obtained:

$$T_{gi} - T_{go} = (T_{gi} - T_b)\Big(1 - exp^{-\frac{h_e A_{gb}}{G_g c_g}}\Big) \tag{4}$$

where the effects due to the heat transfer from gas to the metal part of the chamber are not considered. So an average value of the metal temperature, T_m, is introduced and Equation (4) is refined taking this heat transfer into account as follows:

$$T_{gi} - T_{go} = \Big(T_{gi} - \frac{T_b + F T_m}{1 + F}\Big)\Big(1 - exp^{-\frac{h_e A_{gb}}{G_g c_g}}\Big) \tag{5}$$

The first contribution of this work is the definition of the new parameter F, that is the ratio between the gas-metal and gas-beans thermal resistances:

$$F = \frac{h_{gm} A_{gm}}{h_e A_{gb}} \tag{6}$$

It depends on the gas to metal and gas to beans heat transfer coefficients, h_{gm} and h_e, and the respective contact areas, A_{gm} and A_{gb}. In [13] the term F is negligible since for the mentioned roasters (rotating-bowl, scoop-wheel, spouted-bed, swirling bed roasters) this term is small. On the contrary in this application the term F is significant and so it has to be considered. Moreover, it is one of the parameters related to the chamber geometry so it is an important term in order to make the model scalable. Of course it requires the knowledge of both chamber and coffee beans dimensions in order to reach our purpose.
The contact area between gas and metal, A_{gm}, is then defined as the sum of the inner surface of the chamber and the total surface of the flaps inside it:

$$A_{gm} = \pi D_{ch}(L_{ch} + (H_{\text{flap}} L_{ch})/S_{\text{flap}} + D_{ch}/2) \tag{7}$$

where D_{ch} and L_{ch} are the diameter and the length of the chamber respectively, S_{flap} and H_{flap} are the step and the height of the flap.

The gas to beans heat transfer area, A_{gb}, depends on the dimensions of the beans, assumed having an average dimension determined experimentally in [16]. The total surface area of the beans is assumed to be $A_b = (M_b/m_b)\pi D_b^2$, where M_b is the total weight of the beans loaded in the chamber, m_b is the weight of a single bean and D_b is the bean diameter. Since the model considers a rotating drum, it is necessary to define new parameters to determine the contact area between beans-metal and beans-gas. At each time instant a portion of the beans is in contact with the metal on the bottom of the drum, while the remaining part is in contact with the gas, pushed by the rotatory movement of the drum. So, calling P_{bm} the percentage of contact area of a single bean to the metal, the contact area between metal and beans A_{bm} is defined as $A_{bm} = A_b P_{bm}$ and consequently the contact area between gas and beans as $A_{gb} = A_b(1 - P_{bm})$.

3.2. Bean temperature

According to [13] the bean temperature variation is given by the following energy balance:

$$\dot{T}_b = \frac{Q_{gb} - Q_{gm} + Q_{bm} + M_{bd}(Q_r + \lambda \dot{X})}{M_{bd}(1 + X)c_b} \tag{8}$$

Briefly, the heat is mainly transferred from the gas to the beans by convection (Q_{gb}), while a small part is transferred from the gas to the metal of the chamber (Q_{gm}), which in turn transfers heat to the beans by conduction (Q_{bm}). The final term of (8) represents the heat produced due to exothermic reactions inside the beans: part of energy is lost, representing the latent heat of vaporisation of the moisture inside the bean.
In the following, each element in Equation (8) is further described. The heat transfer rate between gas and beans is defined as:

$$Q_{gb} = G_g c_g (T_{gi} - T_{go}) \tag{9}$$

the heat transfer rate between gas and metal is:

$$Q_{gm} = \frac{F(h_e A_{gb}(T_b - T_m) + Q_{gb})}{1 + F} \tag{10}$$

and the heat transfer rate between metal and beans is:

$$Q_{bm} = h_{bm} A_{bm} (T_m - T_b) \tag{11}$$

where h_{bm} is the metal to beans heat transfer coefficient. Moreover, M_{bd} is the mass of dry beans in the chamber, Q_r is the exothermic heat production, λ is the latent heat of vaporization of beans moisture and $c_b = (c_s + c_w X)/(1 + X)$ is the specific heat capacity of coffee beans, as expressed in [13], where $c_s = 1.099 + 0.007T_b$ is the partial heat capacity of bean solids, c_w is the partial heat capacity of water and X is the beans moisture content.

3.3. Metal temperature

The metal temperature variation is defined as [13]:

$$\dot{T}_m = \frac{Q_{gm} - Q_{bm} + Q_e}{M_m c_m} \tag{12}$$

Basically, T_m increases thanks to the heat transfer from the gas while it decreases transferring heat to the beans. The heat transfer from sources external to the chamber, Q_e, in this case is negligible since the model assumes that there is no leak in the roasting chamber. M_m and c_m are the mass and specific heat capacity of the metal, respectively.

3.4. Moisture loss

A semi-empirical relation between X and T_b is defined to model water evaporation during the roasting process, through an Arrhenius-type equation [13], where k_1 and k_2 are semi-empirical parameters:

$$\dot{X} = -\frac{k_1}{D_b^2} exp^{-\frac{k_2}{T_b + 273.15}} \tag{13}$$

3.5. Exothermic roasting reactions

After the evaporation, heat is generated by exothermic reactions as reported in [12]. This effect is modelled as follows [13]:

$$Q_r = A\frac{H_{et} - H_e}{H_{et}} exp^{-\frac{H_a}{R(T_b+273.15)}} \tag{14}$$

where H_{et} is the total reaction heat, H_e is the reaction heat produced thus far, H_a is the reaction activation energy and R is the gas costant. Reactants are consumed during the process and the concentration of the remaining ones is proportional to $(H_{et} - H_e)/H_{et}$, called $\bar{H}$. The rate of the reactions is proportional to $\bar{H}$ and to the coefficient of the Arrhenius equation, called A.

3.6. Model equations

Starting from these considerations, the model dynamic is represented by four states, two inputs and one output, as listed below:

- $x_1 = T_b$: temperature of the coffee bean inside the roasting chamber in Celsius;
- $x_2 = T_m$: temperature of the metal chamber;
- $x_3 = X$: moisture content of the coffee bean;
- $x_4 = H_e$: amount of heat produced per kilogram of dry coffee thus far;
- $u_1 = G_g$: mass flow rate of the gas at the inlet of the roasting chamber;
- $u_2 = T_{gi}$: temperature of the gas at the inlet of the roasting chamber;
- $y = T_{go}$: temperature of the gas at the outlet of the roasting chamber.

The differential equations representing the model are:

$$\dot{x}_1 = \frac{Q_{gb} - Q_{gm} + Q_{bm} + M_{bd}(Q_r + \lambda\dot{x}_3)}{M_{bd}(1 + x_3)c_b} \tag{15a}$$

$$\dot{x}_2 = \frac{Q_{gm} - Q_{bm} + Q_e}{M_m c_m} \tag{15b}$$

$$\dot{x}_3 = \frac{k_1}{D_b^2} exp^{-\frac{k_2}{x_1+273.15}} \tag{15c}$$

$$\dot{x}_4 = A\frac{H_{et} - x_4}{H_{et}} exp^{-\frac{H_a}{R(x_1+273.15)}} \tag{15d}$$

$$y = \left(u_2 - \frac{x_1 + Fx_2}{1 + F}\right)\left(1 - exp^{-\frac{h_e A_{gb}(1+F)}{u_1 c_{pg}}}\right) \tag{15e}$$

It is important to notice that M_{bd} has been defined is this work by $M_b/(1 + x_3(0))$, where M_b is the weight of the green beans coffee batch, so that also this parameter contributes to the scalability of the model.

4. Experimental setup

The standard equipment of an industrial roasting plant can provide only one of the signals described by the proposed model: the inlet gas temperature $T_{gi} \equiv u_2$. In order to collect the data required for the model identification, the inlet gas mass flow rate $G_g \equiv u_1$ has to be measured.
The bean temperature is the main measure of the whole process, so every plant is equipped with a temperature sensor that tries to measure the bean temperature. Of course this should be modelled to consider delays due to the sensor. So a well known sensor model proposed in [13] is included in order to allow an input-output identification.

4.1. Flow sensor

The measure of G_g was originally not available so that a Pitot tube and a thermocouple were placed in the centre of the inlet pipe of the roasting chamber to obatin the needed measure. Further detail of the placement of the sensor can be found in [4] and [19]. As described in [15], the required measure is given by:

$$G_g = S\sqrt{2\rho_0 \Delta p \frac{273.15}{T + 273.15}} \tag{16}$$

where S is the section of the pipe, ρ_0 is the air density (assumed 1.275 kg/m^3), Δp is the pressure difference measured by the Pitot tube and T is the thermocouple measurement expressed in Celsius degrees.

4.2. Measured bean temperature

The bean temperature is usually measured through thermocouples. Since coffee beans are not good conductors, there is a difference between the effective bean temperature T_b and the measured one T_a. In [13] this difference is modelled as:

$$\dot{T}_a = K_t(T_b - T_a) \tag{17}$$

5. Parameters estimation

Most of the model parameters described in Section 3 are specific of the roasting plant and directly measurable on it or can be obtained from well known physical expressions. On the contrary, three parameters, h_{gm}, h_{bm} and P_{bm}, are not measurable and have to be identified from the data. In this work, an automatic identification procedure to define the optimal values of these parameters, h^*_{gm}, h^*_{bm} and P^*_{bm}, is proposed.

5.1. Data collection

Through the setup described in Section 4, two datasets were collected from two plants of different sizes. The first dataset, *dataset-I*, was collected on a 120 kg roaster and composed of $N = 5$ batches; the second one, *dataset-V*, was collected on a 360 kg roaster and composed of 2 batches. *Dataset-I* was selected as identification set and *dataset-V* as validation set. In particular, each dataset is composed by the inlet gas temperature (u_1), inlet gas mass flow rate (u_2) and the measured bean temperature (T_a).

The extended model (15a)-(15d), (17) is used to generate the bean temperature prediction $\hat{T}_a$ in all the batches of the two datasets. In particular, all the simulations share the same initialization: $x_1(0) = 30$ since the beans are at environmental temperature, $x_2(0) = 121$ as defined in [13], $x_3(0) = 0.1$ by hypothesis, $x_4(0) = 0$ since at the beginning there is no evaporation heat and $\hat{T}_a(0) = T_a(0)$.

5.2. Optimization problem

The goal of the optimization is to find the optimal parameters to match as much as possible the real measure of the coffee bean temperature with the simulated one. In order to do this, the cost function is defined as the Sum of Square Residuals (SSR) between the simulated data vector ($\hat{Y} = \hat{T}_a$) and the real one ($Y = T_a$). SSR is a function of the vector $\theta = [h_{gm}\ h_{bm}\ P_{bm}]'$ used to generate the predictions:

$$SSR^j(\theta) = \sum_{i=1}^{n^j} (\widehat{Y_i^j}(\theta) - Y_i^j)^2 \tag{18}$$

where $\widehat{Y_i^j}(\theta)$ and Y_i^j are the i^{th} samples of the predicted data obtained with a specific θ and of the real measurements respectively, and n^j is the length of the j-th batch of the *dataset-I*.
The optimization problem is then defined as:

$$\begin{aligned} \theta^* &= \arg\min_\theta \textstyle\sum_{j=1}^{N} SSR^j(\theta) \\ &\text{subject to } \theta_{LB} \leq \theta \leq \theta_{UB} \end{aligned} \tag{19}$$

Table 1: Parameters identified on *Dataset-I* with the boundary conditions used in the optimization.

Parameter	Unit	θ_{LB}	θ_{UB}	Optimized value
h_{gm}	$[W/m^2K]$	0.01	0.35	0.0100
h_{bm}	$[W/m^2K]$	0.01	0.35	0.0254
P_{bm}	$[\%]$	0.5	0.8	0.5793

Table 2: Performance indexes.

MAE	MPE	FIT	ρ
$\frac{\sum_{i=1}^{n} \lvert Y_i - \hat{Y}_i \rvert}{n}$	$\frac{100}{n} \sum_{i=1}^{n} \left(\frac{Y_i - \hat{Y}_i}{Y_i} \right)$	$100 \cdot \left(1 - \frac{\lVert \hat{Y} - Y \rVert}{\lVert Y - \overline{Y} \rVert} \right)$	$\frac{\sum_{i=1}^{n} (Y_i - \overline{Y})(\hat{Y}_i - \overline{\hat{Y}})}{\lVert Y_i - \overline{Y} \rVert \cdot \lVert \hat{Y}_i - \overline{\hat{Y}} \rVert}$

Table 3: Performance obtained during training on *Dataset-I* (120 kg) used to calculate the model parameters.

Batch	n	SSR [°C^2]	MAE [°C]	MPE [%]	FIT [%]	ρ
1	26	53.481	4.623	3.722	85.826	0.991
2	25	60.618	5.318	4.422	81.337	0.986
3	26	70.059	8.049	5.846	77.007	0.987
4	26	89.223	10.805	7.661	69.183	0.982
5	33	98.574	8.326	6.979	70.953	0.990
Average		74.391	7.424	5.726	76.861	0.987

Table 4: Performance obtained during validation on *Dataset-V* (360 kg) used to validate the scalability property of the model.

Batch	n	SSR [°C^2]	MAE [°C]	MPE [%]	FIT [%]	ρ
1	28	74.967	8.675	5.416	70.250	0.990
2	28	57.631	5.818	3.910	80.727	0.991
Average		66.299	7.246	4.663	75.489	0.991

with $\theta^*, \theta \in \mathbb{R}^{1\times3}$, where N is the number of datasets used in identification, $\theta_{LB}, \theta_{UB} \in \mathbb{R}^{1\times3}$ are the boundary conditions (see Table 1) defined by practical experience interviewing company experts.
During the optimization, the SSR is minimized through an optimization algorithm solved in MATLAB using the `GlobalSearch` function initialized with $\theta_0 = [0.01\ 0.01\ 0.5]'$.

6. Results

The optimization has been run on *dataset-I* and validated on *dataset-V*. The optimized parameters are reported in Table 1 along their boundaries.

6.1. Model validation

The validation is performed simulating the model and comparing the obtained results with the real data of *dataset-V*. Then, the quality of the model is evaluated using the performance indexes in Table 2 [9], where Y are the real data, $\hat{Y}$ the predicted ones of length n and $\overline{Y}$, $\overline{\hat{Y}}$ are their respective mean values. The index calculation is made on two batches and the results are shown in Tables 3 and 4.

6.2. Discussion

The main goal of this work is to verify whether the proposed model, identified on data collected from a 120 kg plant, can be used to describe the temperature profile acquired on a different plant with a good level of approximation.

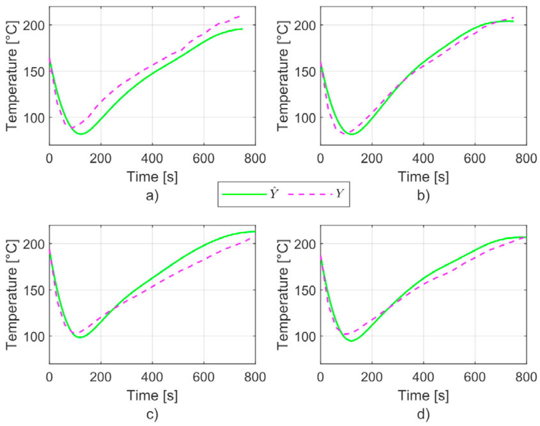

Fig. 2: Temperature profiles a) *dataset-I* batch 4, b) *dataset-I* batch 1, c) *dataset-V* batch 1, d) *dataset-V* batch 2. The simulated values Y_{sim} (green line) are compared with the real ones Y (pink dashed line). For both the datasets the worst (left) and the best (right) cases are reported.

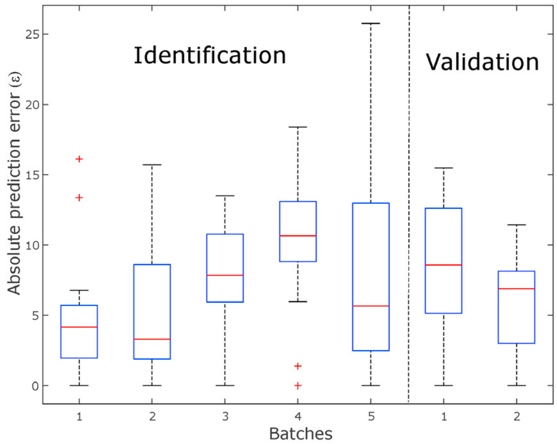

Fig. 3: Absolute error distribution over identification and validation datasets.

Table 5: Parameters of the model. On the left, fixed parameters depending on the process. On the right, scalable parameters depending on the machine geometry.

Fixed Parameter	Value	Unit
A	116200	[kJ/kg]
c_m	0.418	[kJ/(kg °C)]
c_w	5	[kJ/(kg °C)]
D_b	$7.65 \cdot 10^{-3}$	[m]
H_a/R	5500	[K]
H_{et}	232	[kJ/kg]
k_1	$4.32 \cdot 10^{-9}$	
k_2	9889	
K_t	0.01	[1/s]
m_b	$1.5 \cdot 10^{-4}$	[kg]
λ	2790	[kJ/kg]

Scalable Parameter	Value		Unit
M_b	120	360	[kg]
D_{ch}	1.24	1.90	[m]
H_{flap}	0.3	0.3	[m]
L_{ch}	1.335	2.04	[m]
M_m	2000	7000	[kg]
Stp_{flap}	0.1	0.1	[m]

As reported in Table 3, the model obtained good results in term of FIT (75.49%) and MPE (4.66%). Comparing the validation results with the identification ones, reported in Table 4, the two sets showed similar performances. In Fig. 2 the worst (left) and the best (right) case obtained in identification (top) and validation (bottom) are reported. To further investigate the portability of the proposed model, the absolute prediction error (ε) observed in the two datasets can be considered. Fig. 3 reports its distribution along the batches in hand. Even if the variability of the identification set seems bigger (as expected taking in hand the different number of batches) the average values look definitely close. A possible way to address this empirical consideration is to compare the overall error distribution occurred over the *dataset-V* (ε_V) with the one over *dataset-I* (ε_I). The first sample moments are really close ($\overline{\varepsilon_I} = 7.4$ and $\overline{\varepsilon_V} = 7.2$) while the second ones show some distance ($s^2(\varepsilon_I) = 31$, $s^2(\varepsilon_V) = 17$)) that can be likely due to the different number of batches.

Although the limited number of batches used in validation, it can be reasonably assumed that the proposed model, identified on the 120 kg plant, produced satisfying results once scaled on a 360 kg plant via the parameters reported in Table 5. It is important to note that in this kind of application the data collection is not a trivial aspect due to the huge dimension of the plant that requires not negligible time and resources (360 kg of coffee).

7. Conclusion

The model of a roasting chamber proposed in this work proves to be usable on plants of different size by scaling only geometrical parameters directly measurable on the roasting plant. The proposed model was obtained merging two detailed models into a well-known physical framework and defining new parameters in order to correlate the model to geometrical characteristics of the plant, making it scalable. The model parameters were identified from a 5-batches dataset collected on a 120 kg plant with reasonable performance. The portability, that represents the main result of this work, was addressed by predicting the behaviour of a different size plant. In particular, the scaled model is able to predict a 2-batches dataset collected on a 360 kg plant with a good performance (FIT = 75.49%, MPE = 4.66%). Future developments currently under study include the modelling of the other components of the plant that influence the chamber process. Once the whole plant is modelled in detail, new intelligent control approaches (e.g. hybrid control) could be explored in order to optimize the roasting process both in terms of efficiency (ecological and productive), predictive maintenance and analytic. Final goal is to build a simulator in order to synthesize and test new complex control approaches [3].

Acknowledgements

This work was partially supported by Brambati SpA. We acknowledge the contribution of Brambati SpA on sharing their process knowledge and providing data to develop this study.

References

[1] Baggenstoss, J., Poisson, L., Luethi, R., Perren, R., Escher, F., 2007. Influence of water quench cooling on degassing and aroma stability of roasted coffee. Journal of Agricultural and Food Chemistry 55, 6685–6691.
[2] Bottazzi, D., Farina, S., Milani, M., Montorsi, L., 2012. A numerical approach for the analysis of the coffee roasting process. Journal of Food Engineering 112, 243 – 252.
[3] Chai, T., 2015. Intelligent feedback control for operation of complex industrial processes, in: 2015 International Conference on Advanced Mechatronic Systems (ICAMechS), pp. 1–3.
[4] Draghi, R., 2018. Model Identification of a Coffee Roasting Plant for the creation of a Virtual Sensor. Master's thesis. University of Pavia, Italy.
[5] Haley, T.A., Mulvaney, S.J., 1995. Advanced process control techniques for the food industry. Trends in Food Science and Technology 6, 103 – 110. doi:https://doi.org/10.1016/S0924-2244(00)88992-X.
[6] Hernndez-Daz, W., Ruiz-Lpez, I., Salgado-Cervantes, M., Rodrguez-Jimenes, G., Garca-Alvarado, M., 2008. Modeling heat and mass transfer during drying of green coffee beans using prolate spheroidal geometry. Journal of Food Engineering 86, 1 – 9.
[7] Incropera, F.P., Lavine, A.S., Bergman, T.L., DeWitt, D.P., 2013. Principles of heat and mass transfer. Wiley.
[8] LiangHui, D., Reeveerakul, N., 2019. Analysis of critical knowledge in a coffee supply chain, in: 2019 Joint International Conference on Digital Arts, Media and Technology with ECTI Northern Section Conference on Electrical, Electronics, Computer and Telecommunications Engineering (ECTI DAMT-NCON), pp. 271–275.
[9] Ljung, L. (Ed.), 1999. System Identification (2Nd Ed.): Theory for the User. Prentice Hall PTR, Upper Saddle River, NJ, USA.
[10] Milani, M., Montorsi, L., Terzi, S., 2017. Numerical analysis of the heat recovery efficiency for the post-combustion flue gas treatment in a coffee roaster plant. Energy 141, 729 – 743.
[11] Prez-Alegra, L., Ciro-Velasquez, H., 2001. Mathematical simulation of parchment coffee drying in a deep bed with airflow reversal. Transactions of the American Society of Agricultural Engineers 44, 1229–1234.
[12] Raemy, A., 1981. Differential thermal analysis and heat flow calorimetry of coffee and chicory products. Thermochimica Acta 43, 229 – 236.
[13] Schwartzberg, H., 2002. Modeling bean heating during batch roasting of coffee beans, in: Engineering and Food for the 21st Century. CRC Press, pp. 901–920.
[14] Thazin, Y., Pobkrut, T., Kerdcharoen, T., 2018. Prediction of acidity levels of fresh roasted coffees using e-nose and artificial neural network, in: 2018 10th International Conference on Knowledge and Smart Technology (KST), pp. 210–215.
[15] Thottathikudy, P.R., 2019. Model Identification of an Industrial Coffee Roasting Plant. Master's thesis. University of Pavia.
[16] Vosloo, J., 2017. Heat and mass transfer model for a coffee roasting process. Master's thesis. North-West University (South Africa), Potchefstroom Campus.
[17] Winjaya, F., Rivai, M., Purwanto, D., 2017. Identification of cracking sound during coffee roasting using neural network, in: 2017 International Seminar on Intelligent Technology and Its Applications (ISITIA), pp. 271–274.
[18] Xu, Y., Shaull, J., Bavar, T., Tan, L., 2018. Smart coffee roaster design with connected devices, in: 2018 IEEE International Conference on Consumer Electronics (ICCE), pp. 1–5.
[19] Zhiqiang Sun, Zhiyong Li, Jianwu Zheng, 2009. Influence of improper installation on measurement performance of pitot tube, in: 2009 International Conference on Industrial Mechatronics and Automation, pp. 53–56.